

Original Article

Inhibition of microRNA-34a alleviates spinal cord injury through regulating anti-apoptotic Bcl-2 protein in rats

Qilong Deng^{1,2}, Yaochi Wu², Yijun Sun²

¹Shanghai University of Traditional Chinese Medicine, Shanghai, China; ²Department of Acupuncture, Tuina and Traumatology, Shanghai Jiao Tong University Affiliated Sixth People's Hospital, Shanghai, China

Received October 26, 2016; Accepted October 27, 2016; Epub January 1, 2017; Published January 15, 2017

Abstract: Spinal cord injury (SCI) is a severe health problem, which causes lifelong disability for patients. The pathophysiological mechanisms of SCI remain unclear. A large number of experiments show that dysregulation of microRNAs (miRNAs) has been found following SCI. The study aimed to investigate the potential role and underlying mechanism of miR-34a following SCI in vivo and in vitro. We firstly downloaded SCI gene expression data GSE19890 from GEO (Gene Expression Omnibus), and miRNAs associated with SCI were screened in the SCI model rat. Then, the effects of miRNA were assessed by silencing and over-expressing the miRNA in vitro and in vivo. In addition, the regulation of Bcl-2 by miR-34a was evaluated by quantitative real-time RT-PCR (qRT-PCR), western blot and luciferase reporter assays. A total of 43 differentially expressed miRNAs were identified. MiR-34a was one of the most significantly upregulated in SCI group comparing with sham group, and its expression was validated in SCI model rat. Function assays showed that inhibition of miR-34a improved locomotor function and SCI recovery attenuated tissue damage and decreased apoptotic cell in SCI model rat, while overexpression of miR-34a had an opposite result. Subsequently, in a SCI cell model (BV-2 cells treated with H₂O₂), we found that the level of miR-34a was also upregulated in a dose-dependent manner. Importantly, downregulation of miR-34a could restore the reduction of cell viability and inhibited cell apoptosis induced by H₂O₂ in murine BV-2 cells. In addition, anti-apoptosis genes Bcl-2, an important regulator of apoptosis, was identified as a direct target of miR-34a. Our present findings suggest that downregulation of miR-34a has a protection effect in SCI by inhibiting cell apoptosis via targeting Bcl-2. Our data indicate that miR-34a may serve as a novel potential target for SCI diagnosis and therapy.

Keywords: Spinal cord injury, apoptosis, microRNA-34a, Bcl-2

Introduction

Spinal cord injury is one of the most common and devastating injuries observed in spine and neurosurgery departments, which is often related to traffic accidents, sports accidents, overburden and falling from a height [1]. SCI can cause permanent disabilities such as paralysis and loss of movement or sensation, and bring heavy burden to society and family. Although many therapies have been explored, all current therapies have demonstrated limited efficacy.

The programmed cell death (apoptosis) is a hallmark of the pathophysiology of secondary injury after SCI [2, 3], which is a gene-controlled process that is stimulated or inhibited by a variety of regulatory factors including several microRNAs (miRNAs) [4]. Previous studies have

shown that SCI alters the transcription levels of a substantial number of genes associated with the regulation of apoptosis [5]. MiRNAs are endogenous, non-coding ~22 nt RNA molecules that negatively regulate gene expression at posttranscriptional level [6, 7]. Recent studies have provided direct evidence of microRNAs involvement in cell apoptosis modulation following SCI [5, 8, 9]. For example, miR-20a was demonstrated to be upregulated early after injury (24 h) that persists at least for 1 week, and silencing of miR-20a is crucial for Ngn1-mediated neuroprotection in SCI, which suggests that miR-20a plays a key role in SCI [8]. In a similar way, miR-486 is upregulated at 7 days after injury and silencing miR-486 after SCI produced a decrease in the magnitude of neuronal death and led to a significant improvement in motor recovery [9]. Thus, understanding the

regulatory roles of additional miRNAs in SCI is essential.

In this study, we observed that miR-34a was one of the most dysregulated miRNAs after SCI, and down-regulation of miR-34a expression had a protection effect in SCI by inhibiting apoptotic cell death in vivo and vitro. Moreover, miR-34a most likely exerts its pro-apoptotic effect by targeting anti-apoptosis genes Bcl-2. Our findings provided new insights into the molecular function of miR-34a on SCI and suggested the potential value of miR-34a for the treatment of SCI.

Materials and methods

Animals

Adult male Sprague-Dawley rats, weighing 180-220 g, were provided by the Center of Experimental Animals, Shanghai Jiaotong University. All animal care, breeding, and testing procedures were approved by the Laboratory Animal Users Committee at Shanghai Jiao Tong University Affiliated Sixth People's Hospital, Shanghai, China. All animals were housed in individual cages in a temperature- and light cycle-controlled environment with free access to food and water.

Establishment of contusion SCI model

Rats were anesthetized with an intraperitoneal injection of 10% chloral hydrate (3 mg/kg). A laminectomy was performed at thoracic vertebra level 10 (T10). Moderate contusion injury was induced using a modified Allen's weight drop apparatus (8 g weight at a vertical height of 40 mm, 8 g×40 mm) on the exposed dura of the spinal cord. Sham injured animals were only subjected to laminectomy [10].

Cell culture and drug treatments

The immortalized murine BV-2 cell line was purchased from the Chinese Academy of Medical Science and cultured in DMEM/F12 (Hyclone, Waltham, MA, USA) supplemented with 10% fetal bovine serum (Hyclone), 100 U ml⁻¹ penicillin and streptomycin in 25-cm² culture flasks at 37°C in a humidified atmosphere with 5% CO₂. Cells were treated with the following drugs. H₂O₂ (30% w/w solution; Sigma, St Louis, MO, USA) was administered to the cells as a 100

mM solution in phosphate-buffered saline (PBS). N-acetyl-L-cysteine (Sigma) was dissolved in water.

Choice of differentially expressed miRNAs list using heat map analysis

We obtained the microarray data from Gene Expression Omnibus (GEO, <http://www.ncbi.nlm.nih.gov/geo/>), and the GEO accession number is GSE19890. The data was generated using the genechip Affymetrix Human Genome U133 Plus 2.0 Array GPL570 (HG-U133_Plus_2), which completely coverage Human Genome U133 Set plus 6500 additional genes for analysis of over 47,000 transcripts.

Observations with adjusted *p*-values ≥ 0.05 were removed, and thus excluded from further analysis. The heat map of the 43 miRNAs most obvious differences was created using a method of hierarchical clustering by GeneSpring GX, version 7.3 (Agilent Technologies, California, United States).

RNA extraction and reverse transcription quantitative PCR

Total RNA was isolated using TRIzol (Invitrogen, CA) and miRNeasy mini kit (Qiagen, West Sussex, UK) according to manufacturer's instructions. Total RNA from each sample was reverse-transcribed to cDNA using the PrimeScript RT reagent Kit (TaKaRa, Tokyo, Japan) and qRT-PCR was performed using the SYBR Premix Ex Taq (TaKaRa, Tokyo, Japan) and miRNA-specific primers for miR-34a (Ribobio, Guangzhou, China). The relative microRNA levels were normalized to U6 expression for each sample. Analyses of gene expression were performed by the 2^{- $\Delta\Delta$ Ct} method.

Cell viability assay

BV-2 cells were seeded in 96-well culture plates with 1×10⁴ cells/well, and incubated at 37°C with 5% CO₂. After treating with 100 μ M of H₂O₂, MTT assay (Amresco, Solon, USA) was performed. Briefly, 20 μ L of MTT solution (5 mg/ml) was added to each well, and the cells were continuously incubated for 4 h. Formazan crystals were then dissolved in 150 μ L DMSO. The optical density (OD) of the wells was measured with a microplate reader (BioTek, Richmond, USA) at 490 nm.

Apoptosis assay

To detect the effects of miR-34a on BV-2 cell apoptosis, the cells (50-60% confluent) were transfected with miR-34a inhibitor or negative control. After treatment, the cells were washed with 1×PBS for threetimes. Then, an Annexin-V FITC-PI Apoptosis Kit (Invitrogen) was applied to determine the apoptotic rate by flow cytometry. This assay employs fluorescein-labeled Annexin-V in concert with propidium iodide (PI) to detect the cells undergoing apoptosis.

Transfection

The cells were plated into six-well plates and grown to 30-50% confluence after 24 hours of incubation and were then transfected with miRNA mimics, miRNA inhibitor and negative control at a final multiplicity of infection of 10 using siLentFect™ Lipid reagent (Life Science Research). The cells were then diluted in DMEM/F12 without serum (GeneChem, Shanghai, China). After 4 h of incubation in a CO₂ incubator at 37°C, the medium was changed to 10% FBS containing DMEM.

Terminal deoxynucleotidyl transferase-mediated biotinylated UTP nick end labeling (TUNEL) staining

Apoptosis cells were detected with the In Situ Cell Death Detection kit, Fluorescein (Roche Applied Science, Indianapolis, IN, USA) according to the manufacturer's protocol. Briefly, 4 mm sections were fixed with 4% paraformaldehyde and incubated with permeabilization solution for 2 min on ice. The negative control sections were incubated only in label solution and the positive control sections were treated with 50 U/ml DNaseI (Sigma) prior to labeling procedures. Then sections were incubated with enzyme solution. Finally, the number of TUNEL positive cells was counted. Each section was counted independently by two observers using a light microscope (×200 magnifications).

BBB score

Locomotor activity was evaluated at 1, 3, 7, 14, 21, and 28 days post-injury using the BBB score, which measured locomotor ability for 4 min. Two independent and well-trained investigators observed the movement and scored the locomotor function according to the BBB scales as described previously. Investigators were

blind to the treatment. The final score of each animal was obtained by averaging the values from both investigators.

Lesion identification by cresyl violet staining

After the final behavioral tests, which occurred 28 days after surgery, the animals were terminally anesthetized and transcardially perfused with 250 mL of 0.9% NaCl (4°C) followed by 500 mL of 4% paraformaldehyde (PFA) (4°C). A 1 cm segment of spinal cord was dissected and post-fixed in the same fixative for 24 h at 4°C. After fixation, the tissue blocks were embedded in paraffin. Transverse sections (10 µm thickness) were taken through the width of the spinal lesion site, and put onto Superfrost Plus Slides. Every 40th section of the lesion site sample was stained with 0.5% cresyl-violet acetate and imaged using a microscope (BH-2; Olympus, NY). Using Image-Pro Plus 6.0 (Media Cybernetics, USA) software, the lesion area and spared tissue area were outlined and quantified. The lesion epicenter was identified as the section with the least amount of spared white matter [10].

Luciferase reporter assay

Dual luciferase assays were conducted in a 24 well plate format. pGL3-Bcl-2 3'UTR report/pGL3-Bcl-2 3'UTR Mutant report + TK100 Renilla report were transfected into 70% confluent BV-2 cells, along with miR-34a mimic, miR-34a inhibitor or each control. After 48-h transfection, firefly and renilla luciferase were quantified sequentially using the Dual Luciferase Assay kit (Promega, USA) following the manufacturer's recommendations.

Western blot analysis

Protein extracts from BV-2 cells were subjected to 10% SDS-PAGE and subsequently transferred to a PVDF membrane. The membrane was blocked with 5% (w/v) nonfat milk and incubated sequentially with the primary antibodies against cleaved caspase 3, cleaved caspase 9, cleaved PARP (rabbit, 1:2000, Abcam, Cambridge, UK), Bcl-2 (rabbit, 1:1000, Santa Cruz Biotechnology) in TBST containing 5% bovine serum albumin overnight at 4°C. Anti-β-actin antibody was used as an internal control. After washing three times with TBST, the membrane was incubated at room temperature for 2 hours with horseradish peroxidase-conjugated

microRNA-34a and spinal cord injury

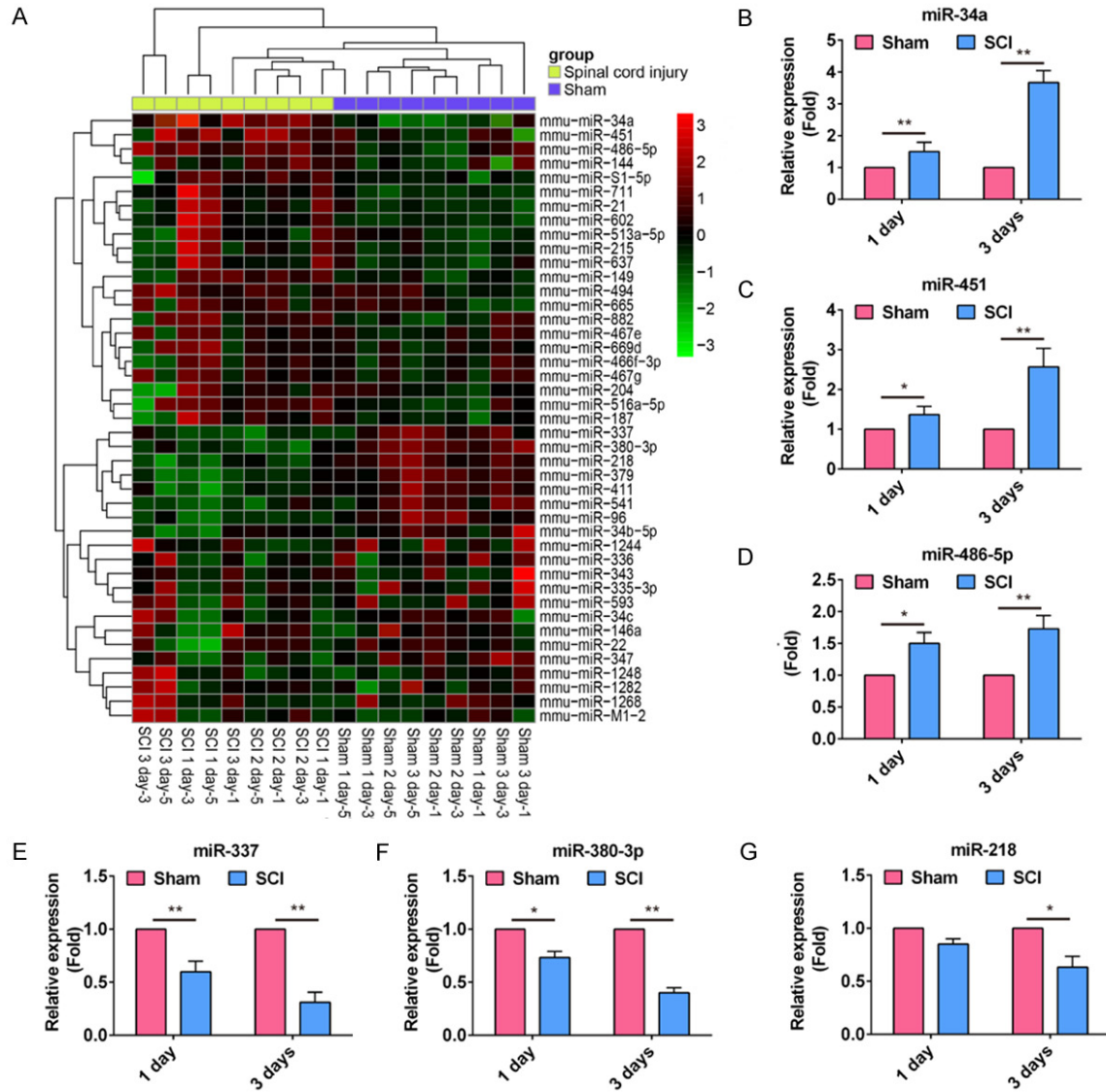


Figure 1. Hierarchical cluster analyses of altered microRNAs (miRNAs) after spinal cord injury in rats. A. Differentially expressed miRNAs in the sham and SCI group, 1 day and 3 days post-injury and their expression data were downloaded from the GEO Profiles (GSE19890). Expression values are represented in shades of red and green indicating expression above and below the median expression value across all samples. B-G. QRT-PCR analysis confirmed the microarray analyses of six miRNAs (miR-34a, miR-451 and miR-486-5p, miR-337, miR-380-3p and miR-218) 1 and 3 days after spinal cord injury. Relative expression indicates changes compared with the sham group at either 1 or 3 days after SCI. Bars represent the mean \pm SD. *P < 0.05; **P < 0.01.

secondary antibody (anti-rabbit, 1:2000, Cell Signaling Technology) diluted with TBST. The detected protein signals were visualized using an enhanced chemiluminescence (ECL) system western blot kit (Thermo Fisher Scientific, Waltham, MA, USA).

Statistical analysis

Statistical analyses were performed with SPSS 13.0 software. The results were evaluated by χ^2 test and the other data were evaluated by

Student's t-test and expressed as the mean \pm SD from three independent experiments. A P-value of less than 0.05 was considered statistically significant.

Results

Expression of miRNAs after SCI in rats

MiRNAs have been reported to regulate apoptosis in many physiological and pathological processes including SCI [4]. According to the

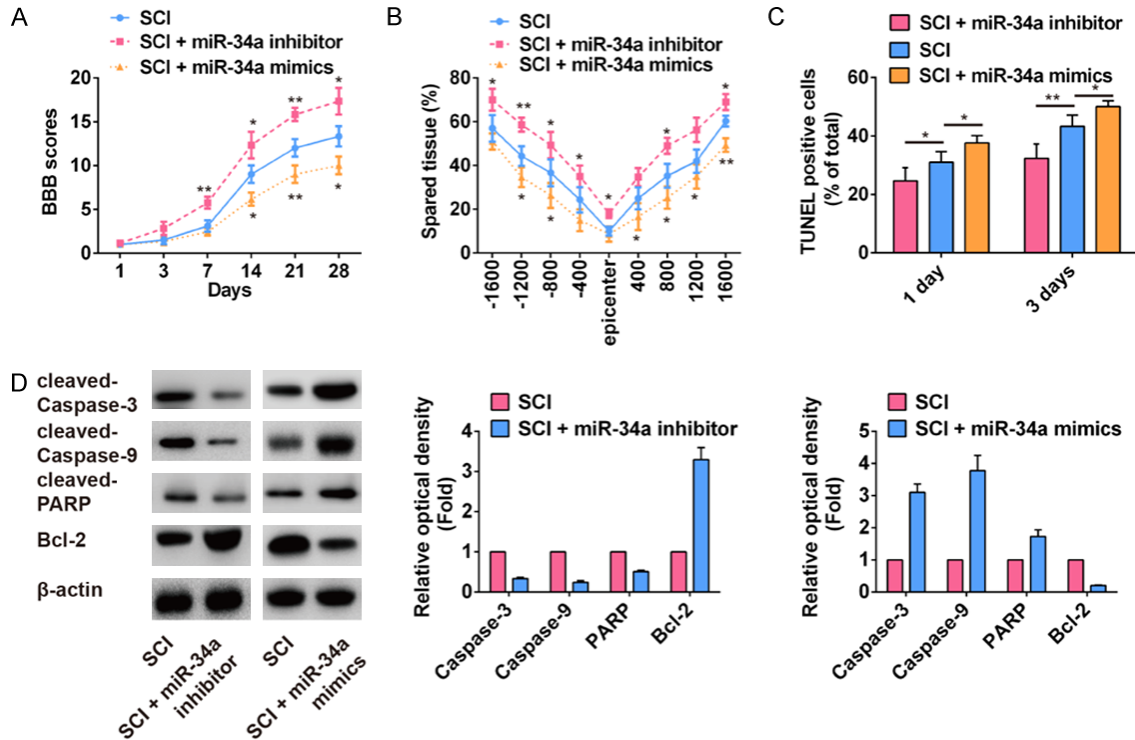


Figure 2. Inhibition of miR-34a improved the functional deficit, attenuated tissue damage and decreased apoptotic cell after SCI. A. Hind limb recovery was assessed from day 1 to day 28 after SCI using BBB Score. Hind limb dysfunction was improved with treatment of miR-34a inhibitor (n = 4) when compared with negative control group (n = 4). B. Quantification of spared tissue within the injury site, and 1600 µm rostral and caudal to the epicenter, 28 days post-injury. C. The miR-34a inhibitor group at 3 days after SCI (n = 4) had a lower proportion of TUNEL-positive cells than did the negative control group (n = 4), whereas miR-34a mimic resulted in an opposite results. D. The levels of apoptosis-related proteins including cleaved caspases 3, cleaved 9, cleaved PARP and Bcl-2 are assessed by Western Blot after treatment with miR-34a mimic or miR-34a inhibitor. *P < 0.05, **P < 0.01 vs. SCI group. Data are presented as mean ± SD from three independent experiments.

heatmap obtained from GEO database under the accession number GSE19890 (Figure 1A), it was found that the expression levels of 43 injury-related miRs were dysregulated in the SCI groups at 1 day and 3 days post-injury, including 25 down-regulated miRNAs and 18 up-regulated miRNAs. We further validated the changes in the levels of six miRNAs including miR-337, miR-380-3p, miR-218, miR-34a, miR-451 and miR-486-5p using qRT-PCR at 1 and 3 post-injury in SCI rat model. These data confirmed that miR-34a, miR-451 and miR-486-5p were over-expressed compared with the sham group, whereas the expression of miR-337, miR-380-3p and miR-218 was decreased (Figure 1B-G). Among the aberrantly expressed miRNAs, miR-34a was chosen as the candidate for further study because previous reports suggested that the overexpression of miR-34a could induce apoptosis [11]. In this study, we observed that miR-34a was the most dysregu-

lated miRNAs after SCI. For these reasons, we focused on miR-34a in SCI for further study.

MiR-34a inhibitor decreased cell apoptosis in SCI model rats

To explore the effect of miR-34a following rat SCI, BBB scores and Cresyl violet staining were used to evaluate the hind limb locomotor activity and spared tissue. As shown in Figure 2A, the locomotor scores increased progressively during the experimental period. The behavioral analysis showed that hind limb dysfunction was improved with treatment of miR-34a inhibitor (n = 3) when compared with negative control group, whereas hind limb dysfunction was exacerbated with treatment of miR-34a mimic from 14 d to 28 d. In addition, compared with the negative control group, miR-34a inhibitor-treated rats had significantly larger spared tissue areas at multiple distances from the lesion epi-

microRNA-34a and spinal cord injury

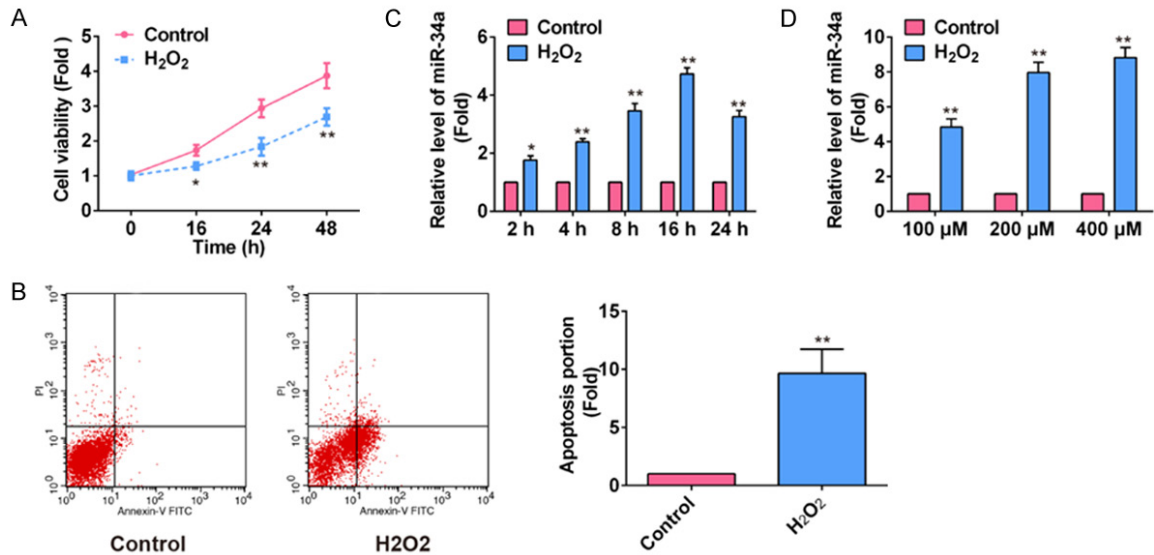


Figure 3. Establishment of SCI cell model in murine BV-2 cell line. A. Murine BV-2 cells were exposed to 100 μM H_2O_2 for 24, 36 and 48 h. The growth of Murine BV-2 cells was measured using an MTT assay. B. Murine BV-2 cells apoptosis after treatment with 100 μM H_2O_2 for 24 hours was assessed. The cells were stained with Annexin V-FITC and PI and subjected to flow cytometric analysis. C. The level of miR-34a was determined by RT-PCR after treatment with 100 μM H_2O_2 for 2, 4, 8, 16 and 24 hours. D. The level of miR-34a was determined by qRT-PCR at H_2O_2 concentrations of 100-400 mM. Data are presented as mean \pm SD from three independent experiments. * $P < 0.05$, ** $P < 0.01$ vs. Control group.

center, while miR-34a mimic-treated rats had opposite results (**Figure 2B**). These dates indicate that miR-34a inhibitor could improve the motor function, whereas miR-34a mimic could exacerbate the injury to the spinal cord.

Moreover, we found that miR-34a inhibitor resulted in a marked decrease in the number of TUNEL positive cells when compared with that of the negative control group at Day 3, while miR-34a mimic resulted in an opposite results (**Figure 2C**). Both caspase-dependent and -independent pathways are known to be involved in the process of apoptosis. Western blot analysis of apoptotic protein expression showed that the upregulation of miR-34a by the mimics increased the expression of caspases 3, 9 and PARP, the key executioners of apoptosis, whereas miR-34a inhibitor decreased the expression of caspases 3, 9, and PARP, which was along with dysregulation of Bcl-2 protein in activated apoptotic pathway (**Figure 2D**). These results suggest that the miR-34a has a protection effect by inhibiting cell apoptosis in SCI model rats.

Establishment of SCI cell model in murine BV-2 cell line

To explore the molecular mechanism by which miR-34a induces apoptosis in SCI, the immor-

talized murine BV-2 cell line was applied as it is reported to share many characteristics with primary microglia. Firstly, the H_2O_2 induced BV-2 cell injury as a model of SCI in vitro was established as previously described [12]. After murine BV-2 cells were exposed to 100 μM H_2O_2 , MTT Assay showed that H_2O_2 significantly reduced cell viability of BV-2 cells in a time-dependent manner (**Figure 3A**). Furthermore, flow cytometry analysis revealed that the apoptotic rate was markedly increased in BV-2 cells treated with 100 μM H_2O_2 (**Figure 3B**). These result together show that a SCI cell model was successfully established.

Furthermore, we found that miR-34a was upregulated after 2 h exposure of H_2O_2 and its expression reached the peak at 16 h (**Figure 3C**). Moreover, the level of miR-34a was increased in a dose-dependent manner at H_2O_2 concentrations of 100-400 μM (**Figure 3D**). Therefore, we used H_2O_2 with the concentration of 100 μM and selected 16 h exposure of H_2O_2 for the following analysis.

MiR-34a inhibitor decreased H_2O_2 -induced apoptosis of BV-2 cells

To evaluate the role of miR-34a in H_2O_2 induced apoptosis in murine BV-2 cells; we knocked

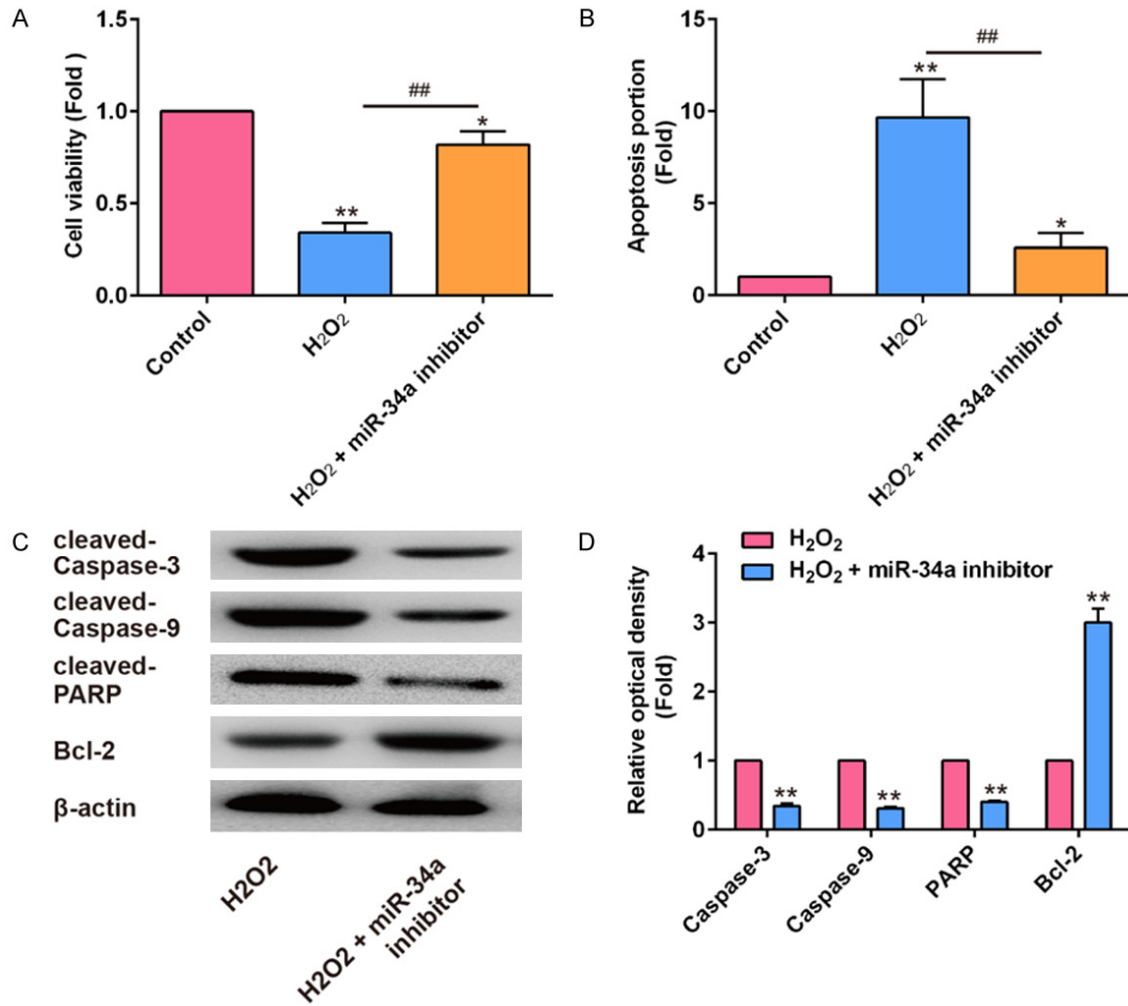


Figure 4. Inhibition of miR-34a alleviates H₂O₂-induced apoptosis of murine BV-2 cells. A. The growth of Murine BV-2 cells was measured using an MTT assay after transfection with miR-34a inhibitor or negative control. Knockdown of miR-34a mitigates the reduction of cell viability induced by H₂O₂ in BV-2 cells. B. The apoptosis of Murine BV-2 cells was measured after transfection with miR-34a inhibitor or negative control. Inhibition of miR-34a blocks H₂O₂-induced apoptosis of BV-2 cells. C. The expressions of cleaved caspases 3, cleaved caspases 9, and cleaved PARP are assessed at 24 h after transfection with miR-34a inhibitor, or inhibitor control in BV-2 cells with H₂O₂ treatment. D. The optical densities of the bands were measured using Image-Pro Plus software. Data are presented as mean ± SD from three independent experiments. *P < 0.05, **P < 0.01 vs. Control group, ##P < 0.01 vs. H₂O₂ group.

down the expression of miR-34a with the specific inhibitor, and then observed the alteration of H₂O₂-induced apoptosis in BV-2 cells. Our data showed that inhibition of miR-34a restored the reduction of cell viability induced by H₂O₂ (Figure 4A). And, knockdown of miR-34a alleviated H₂O₂-induced apoptosis of BV-2 cells (Figure 4B). Moreover, we observed that inhibition of miR-34a enhanced the level of Bcl-2 and reduced the levels of cleaved caspases 3, 9, and PARP in BV-2 cells treated with H₂O₂ (Figure 4C and 4D). These results indicate miR-34a inhibitor functions to attenuate apoptosis during microglia cell injury.

Bcl-2 was the target gene of miR-34a

To explore the underlying molecular mechanism(s) through which miR-34a induced BV-2 cell apoptosis, we performed a bioinformatics analysis using TargetScan and PicTar to predict potential target genes of miR-34a. The predicted binding sites for miR-34a in the Bcl-2 sequence are illustrated in Figure 5A. To experimentally validate whether Bcl-2 was a direct target of miR-34a, a luciferase assay was performed in BV-2 cells. As shown in Figure 5B, miR-34a knockdown caused a clear increase in relative luciferase activity, whereas activity did

microRNA-34a and spinal cord injury

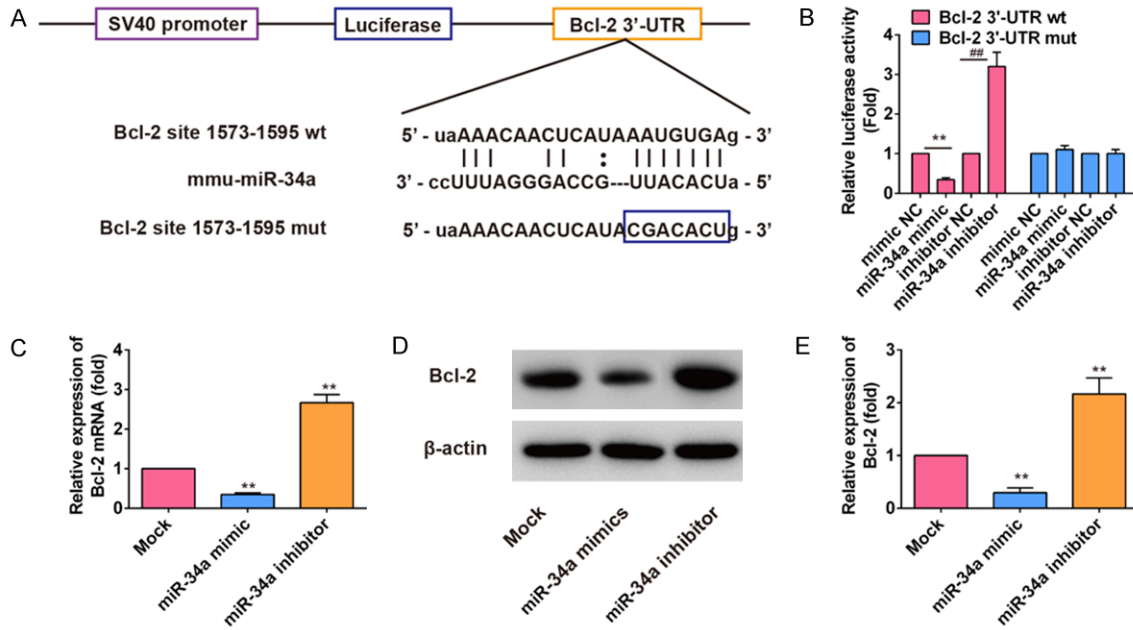


Figure 5. MiR-34a directly targets Bcl-2 in BV-2 cells. **A.** Schema of the firefly luciferase reporter constructs for the Bcl-2, indicating the interaction sites between miR-34a and the 3'-UTRs of the Bcl-2. **B.** Luciferase activities. Murine BV-2 cells were co-transfected with firefly luciferase constructs containing the Bcl-2 wild-type or mutated 3'-UTRs and miR-34a mimic, mimic NC, miR-34a inhibitor or inhibitor NC, as indicated (n = 6). **C.** The mRNA levels of Bcl-2 after treatment with miR-34a mimic or miR-34a inhibitor (n = 6). **D.** The protein expression of Bcl-2 after treatment with miR-34a mimic or miR-34a inhibitor (n = 6). **E.** The optical densities of the bands were measured using Image-Pro Plus software. Data are presented as mean ± SD from three independent experiments. **P < 0.01 vs. Mock group or mimic NC group, ###P < 0.01 vs. inhibitor NC group.

not drop at all in the mutant 3'UTR reporter, indicating that functionality depends on the intact seed sequence. In addition, qRT-PCR and western Blot analysis showed that miR-34a overexpression decreased the levels of Bcl-2 mRNA (**Figure 5C**) and protein expression in BV-2 cells (**Figure 5D, 5E**). These results indicated that Bcl-2 was a direct target of miR-34a in BV-2 cells.

Discussion

In the present study, we found that inhibition of miR-34a improved functional recovery and showed strong anti-apoptotic effect in a rat SCI model. Furthermore, we experimentally confirmed that miR-34a inhibitor exerted its anti-apoptotic effect by targeting Bcl-2 in the BV-2 cells. Thus, tracking the knockdown of miR-34a may be a useful strategy for enhancing neural cell functional recovery after SCI.

Recent researches show that many miRNAs are found in the central nervous system (CNS) and play important roles in regulating proliferation

and differentiation of neural stem cells (NSCs) [8, 13, 14]. For example, miR-134 and miR-184 have been demonstrated to regulate neural progenitor maintenance and proliferation. However, there is only limited research on the role of individual SCI-associated miRNA. Previous research found that miR-133b improved functional recovery after SCI in mice [15] and adult zebrafish [16]. In the present study, we obtain miRNA expression profiles from GEO database under the accession number GSE19890. Based on the results observed with the microarray, six miRNAs (miR-337, miR-380-3p and miR-218, miR-34a, miR-451 and miR-486-5p) were further confirmed by qRT-PCR analysis. Among the six miRNAs we investigated, miR-34a was the most dysregulated miR after SCI. Our data imply its potential role in SCI. In this study, we aimed to clarify the function and molecular mechanism of miR-34a in the pathophysiology of SCI.

Previous studies have found that the miR-34 family, especially miR-34a was rich in the brain, and the abnormal expression of 34a could

reduce apoptosis. For example, Jiang et al. found that miR-34a was markedly upregulated due to ketamine administration and knock-down of miR-34a reduced hippocampal apoptosis [17]. A study from Welch et al. showed that miR-34a functions as a potential tumor suppressor by inducing apoptosis in the neuroblastoma cell lines [18]. Furthermore, inactivation of miR-34a strongly attenuates p53-mediated apoptosis in cells exposed to genotoxic stress, whereas overexpression of miR-34a mildly increases apoptosis [19]. In this study, we showed that miR-34a was upregulated in SCI model rats and knockdown of miR-34a could improve the motor function and attenuate tissue damage. Moreover, the levels of apoptosis-related proteins, cleaved caspase-3, cleaved caspase-9 and cleaved PARP were decreased significantly by miR-34a inhibitor treatment in rat SCI model, whereas the levels of Bcl-2 was increased. To further confirm the anti-apoptotic effect of miR-34a inhibitor in SCI in vitro, we used H₂O₂-treated murine BV-2 cells. According to the results, downregulation of miR-34a restored the cell viability induced by H₂O₂ and inhibited apoptosis induced by H₂O₂ in BV-2 cells. These results indicate that miR-34a knockdown has a protection effect in vivo and in vitro by inhibiting neuronal cell death.

One miRNA can target hundreds of mRNAs. As a result, to further study the downstream target is very critical in understanding the regulatory mechanisms of miRNAs in defined function [20]. Bcl-2 is an anti-apoptotic protein primarily expressed in mitochondria which prevents caspase-9 activation through an interaction with Apaf-1. Duan J et al. found that miR-34a inhibited cell proliferation and induced cell apoptosis of glioma cells via targeting of Bcl-2. Recent study demonstrated that miR-34a led to the abnormal apoptosis in Alzheimer's disease (AD) through regulating the expression of Bcl-2 [21]. In this study, miR-34a could regulate the expression of Bcl-2, which results in the alteration of the level of cleaved caspase-3, cleaved caspase-9 and cleaved PARP. Furthermore, Bcl-2 was identified as a direct target by luciferase assay. These results indicate that miR-34a induced apoptosis in BV-2 cells mainly by suppressing Bcl-2 expression.

In conclusion, a set of miRNAs is frequently aberrantly expressed in SCI model rat. Among them, miR-34a dysregulation contributes to

SCI. Moreover, miR-34a most likely exerts its pro-apoptotic effect by targeting Bcl-2. This finding suggests that miR-34a is a novel therapeutic target, which may potentially allow us to develop additional therapeutic strategies for the treatment of SCI.

Acknowledgements

This study was supported by the Foundation from important clinical projects supported by Shanghai Chinese medicine, traditional Chinese and Western Medicine (ZY3-JSFC-1-1008).

Disclosure of conflict of interest

None.

Address correspondence to: Yaochi Wu, Department of Acupuncture, Tuina and Traumatology, Shanghai Jiao Tong University Affiliated Sixth People's Hospital, Room 301, 145 Ping Ji Residential Quarter, Minhang District, Shanghai 200233, China. Tel: +86-21-24058567; E-mail: wuyaochi-yc@163.com

References

- [1] Krassioukov A, Eng JJ, Warburton DE, Teasell R; Spinal Cord Injury Rehabilitation Evidence Research Team. A systematic review of the management of orthostatic hypotension after spinal cord injury. *Arch Phys Med Rehabil* 2009; 90: 876-885.
- [2] Liu C, Shi Z, Fan L, Zhang C, Wang K and Wang B. Resveratrol improves neuron protection and functional recovery in rat model of spinal cord injury. *Brain Res* 2011; 1374: 100-109.
- [3] Yin X, Yin Y, Cao FL, Chen YF, Peng Y, Hou WG, Sun SK and Luo ZJ. Tanshinone IIA attenuates the inflammatory response and apoptosis after traumatic injury of the spinal cord in adult rats. *PLoS One* 2012; 7: e38381.
- [4] Wang Z. MicroRNA: a matter of life or death. *World J Biol Chem* 2010; 1: 41-54.
- [5] Aimone JB, Leasure JL, Perreau VM, Thallmair M; Christopher Reeve Paralysis Foundation Research Consortium. Spatial and temporal gene expression profiling of the contused rat spinal cord. *Exp Neurol* 2004; 189: 204-221.
- [6] Kosik KS. The neuronal microRNA system. *Nat Rev Neurosci* 2006; 7: 911-920.
- [7] Krichevsky AM. MicroRNA profiling: from dark matter to white matter, or identifying new players in neurobiology. *ScientificWorldJournal* 2007; 7: 155-166.
- [8] Jee MK, Jung JS, Im YB, Jung SJ and Kang SK. Silencing of miR20a is crucial for Ngn1-

microRNA-34a and spinal cord injury

- mediated neuroprotection in injured spinal cord. *Hum Gene Ther* 2012; 23: 508-520.
- [9] Jee MK, Jung JS, Choi JI, Jang JA, Kang KS, Im YB and Kang SK. MicroRNA 486 is a potentially novel target for the treatment of spinal cord injury. *Brain* 2012; 135: 1237-1252.
- [10] Hu JZ, Huang JH, Zeng L, Wang G, Cao M and Lu HB. Anti-apoptotic effect of microRNA-21 after contusion spinal cord injury in rats. *J Neurotrauma* 2013; 30: 1349-1360.
- [11] Zhao Y, Pogue AI and Lukiw WJ. MicroRNA (miRNA) signaling in the human CNS in sporadic alzheimer's disease (AD)-novel and unique pathological features. *Int J Mol Sci* 2015; 16: 30105-30116.
- [12] Yu DS, Lv G, Mei XF, Cao Y, Wang YF, Wang YS and Bi YL. MiR-200c regulates ROS-induced apoptosis in murine BV-2 cells by targeting FAP-1. *Spinal Cord* 2014; [Epub ahead of print].
- [13] Qi Y, Zhang M, Li H, Frank JA, Dai L, Liu H and Chen G. MicroRNA-29b regulates ethanol-induced neuronal apoptosis in the developing cerebellum through SP1/RAX/PKR cascade. *J Biol Chem* 2014; 289: 10201-10210.
- [14] Lagos-Quintana M, Rauhut R, Yalcin A, Meyer J, Lendeckel W and Tuschl T. Identification of tissue-specific microRNAs from mouse. *Curr Biol* 2002; 12: 735-739.
- [15] Theis T, Yoo M, Park CS, Chen J, Kugler S, Gibbs KM and Schachner M. Lentiviral delivery of miR-133b improves functional recovery after spinal cord injury in mice. *Mol Neurobiol* 2016; [Epub ahead of print].
- [16] Yu YM, Gibbs KM, Davila J, Campbell N, Sung S, Todorova TI, Otsuka S, Sabaawy HE, Hart RP and Schachner M. MicroRNA miR-133b is essential for functional recovery after spinal cord injury in adult zebrafish. *Eur J Neurosci* 2011; 33: 1587-1597.
- [17] Jiang XL, Du BX, Chen J, Liu L, Shao WB and Song J. MicroRNA-34a negatively regulates anesthesia-induced hippocampal apoptosis and memory impairment through FGFR1. *Int J Clin Exp Pathol* 2014; 7: 6760-6767.
- [18] Welch C, Chen Y and Stallings RL. MicroRNA-34a functions as a potential tumor suppressor by inducing apoptosis in neuroblastoma cells. *Oncogene* 2007; 26: 5017-5022.
- [19] Raver-Shapira N, Marciano E, Meiri E, Spector Y, Rosenfeld N, Moskovits N, Bentwich Z and Oren M. Transcriptional activation of miR-34a contributes to p53-mediated apoptosis. *Mol Cell* 2007; 26: 731-743.
- [20] Baek D, Villen J, Shin C, Camargo FD, Gygi SP and Bartel DP. The impact of microRNAs on protein output. *Nature* 2008; 455: 64-71.
- [21] Wang X, Liu P, Zhu H, Xu Y, Ma C, Dai X, Huang L, Liu Y, Zhang L and Qin C. MiR-34a, a microRNA up-regulated in a double transgenic mouse model of Alzheimer's disease, inhibits bcl2 translation. *Brain Res Bull* 2009; 80: 268-273.